1   **Methods to assess neuronal primary cilia electrochemical signaling.**

2

3   Paul G. DeCaen and Louise F. Kimura*

4   Northwestern University, Feinberg School of Medicine, Department of Pharmacology, Chicago,

5   Illinois

6

7   *indicates corresponding author

8   louise.kimura@northwestern.edu

9

10

11   **Running title:** Methods to study neuronal primary cilia signaling.

12

13   **Keywords 5-7:** primary cilia, electrophysiology, calcium sensor, cAMP, serotonin receptor type

14   6, neuronal ciliopathies

15

16

17 **Abstract**

18 Primary cilia are polymodal sensory organelles which project from the apical side of polarized
19 cells. They are found in all brain hemispheres but are most pronounced in neurons which
20 comprise the granular layers of the hippocampus and cerebellum. Pathogenic variants in genes
21 which encode primary cilia components are responsible for neuronal ciliopathies— a group of
22 central nervous system disorders characterized by neurodevelopmental conditions such as
23 intellectual disability, seizure, ataxia, and sensory deficits. In the hippocampus, neuronal primary
24 cilia form chemical synapses with axons and their membranes are populated with unique sets of
25 ion channels and G protein-coupled receptors (GPCRs). Primary cilia are small and privileged
26 compartments that are challenging organelles to study. In detail, we describe cilia
27 electrophysiology methods and the use of cilia-specific fluorescent sensors to assay neuronal
28 polycystin channel function and serotonergic receptor signaling, respectively. These tools allow
29 researchers to assay calcium, cAMP and channel-related signaling pathways in isolated neurons
30 in real time and in semi-quantitative terms, while enhancing our understanding of this
31 understudied organelle and its dysregulation in ciliopathy disease states.

1 Introduction

Neuronal primary cilia act as specialized sensory and signaling hubs— receiving and processing signals from the external environment to coordinate unique forms of electrochemical communication[1-3]. Ciliogenesis in most types of neurons occurs during G0 and G1 phases of the cell cycle, utilizing mitotic microtubule machinery which are dynamically regulated[4]. The mother centriole migrates to the apical surface of the neuron, forming the basal body of the primary cilium and the nucleation site of microtubules of the internal scaffolding structure known as the axoneme array (9+0). Once fully developed, the primary cilium extends 2–12 µm from the apical surface of the neuronal plasma membrane, with a diameter of less than 500 nm[5-8]. At the neuronal primary cilia-cell junction, the basal body partners with the BBSome— a protein complex which, along with diffusion barriers present at the ciliary base, give the organelle its privileges status and unique composition. Once inside the cilia, the intraflagellar transport (IFT) system shuttles ciliary proteins and other cargo along the axoneme via motor proteins[9,10]. Here, critical cilia signaling pathways such as Hedgehog and Wnt that are vital for maintaining neuronal polarity, cell fate determination, and tissue patterning are established[11-14]. Primary cilia from hippocampal neurons form serotonergic synapses with axons on brain stem neurons (axo-ciliary synapse), which modulates the post synaptic neuron's epigenetic state through $G\alpha q11$-Rho mediated chromatin accessibility changes[15]. In addition, neuronal primary cilia in disparate locations within the central nervous system express unique GPCRs, such as SSTR3 (cerebral cortex, hippocampus, hypothalamus, cerebellum, amygdala), MC4R (hypothalamus, brainstem) and 5-HT6R (hippocampus, cerebral cortex, striatum)[16-18]. In various regions within the CNS, SSTR3 is coupled to $G\alpha i$, while MC4R signals through $G\alpha s$ and crosstalks with other ciliary proteins such as ADCY3[19,20]. Whereas 5-HT6R signals through $G\alpha s$ but also promotes $G\alpha q11$-Rho mediated signaling[15,20-22]. These cilia-specific signals regulate a wide range of physiological functions from appetite control; metabolic regulation; cognitive processes and sensory perception. Disruption of GPCRs and channels in the cilium can lead to significant brain developmental disorders and animal neurophenotypes, underscoring their critical role in neuronal function[23,24].

The importance of the primary cilia in human health is highlighted by more than 35 congenital diseases called "ciliopathies", which impact the development of organ systems such as the kidney, brain, heart and eye[25,26]. A subset of these syndromes can be classified as neuronal ciliopathies as the gene variants cause defects in the structure or function of primary cilia in neurons (**Table 1**)[23,27]. For example, Joubert syndrome and Bardet-Biedl syndrome are caused by variants in the genes encoding for cilia assembly components— such as centrosomal CEP120 and BBS proteins, and the GTPase ARL13B[28]. These syndromic diseases primarily impact the development of the central nervous system but also have comorbidities affecting organ systems outside of the brain. Developmental defects are common amongst individuals with neuronal ciliopathies, such as polydactyly (extra digits on hands and toes) and *situs inversus* or *totalis* (inverted positioning of body organs)[29]. In addition, common comorbidities shared by neuronal ciliopathies are polycystic kidney disease (PKD) and other renal defects such as nephronophthisis, but the reason for this is not known[26,30]. However, since the autosomal dominant form of PKD (ADPKD) is caused by gene variants in renal cilia calcium channel subunits (PKD1 and PKD2*),* and since other ciliopathy variants impact Ca^{2+} effectors (e.g. CEP 290) share

75 renal cyst comorbidities— localized ciliary Ca^{2+} dysregulation might be a unifying disease-causing
76 mechanism observed in these conditions[31-35].

77 Our understanding of the primary cilia in neurons has been restricted by the limitations of
78 traditional tools to assess dynamic chemical changes within this privileged organelle.
79 Methodologies such as immunofluorescence of fixed samples only capture static changes in cilia
80 signaling. Neuronal primary cilia do not load with standard calcium dyes (e.g., Fura) or cAMP
81 fluorescent reporters (e.g., unconjugated cADDis) where their diffusion is limited to the soma,
82 axon, and dendritic compartments. To address this, several groups have developed cilia-localized
83 ratiometric Ca^{2+} sensors, and reporters that enhance fluorescence intensity in response to ciliary
84 cAMP concentration (**Table 2**)[36-38]. Here, we describe methods for the deployment of Ca^{2+} and
85 cAMP sensors, both in isolation and in combination, to assess cell signaling in primary cilia of
86 cultured hippocampal neurons. Although it is established that neuronal primary cilia are richly
87 populated with polycystin transient receptor potential (TRP) channels encoded by PKD2L1— their
88 ion channel activity cannot be assessed by voltage clamping the soma or cell body membranes[39].
89 To address this, we provide experiment details to directly record neuronal primary cilia PKD2L1
90 channels aided by the expression of genetically encoded fluorescent reporters (**Table 2**)[6,40-42].
91 Outcomes proved a methodological toolbox to studying ciliary chemical and electrical activity in
92 real time to understand the basic biology of this understudied organelle and its dysregulation in
93 ciliopathy disease states.
94

95 **2 Material and methods**
96

97 *2.1 Hippocampal neurons primary culture.*
98 All mice utilized were housed in AAALAC-approved Center for Comparative Medicine
99 (CCM) at Northwestern University, Feinberg School of Medicine. All procedures with mice were
100 in accordance with the recommendations of the Panel on Euthanasia of the American Veterinary
101 Medical Association. Animals were maintained in temperature-controlled rooms on a 12 h
102 day/light cycle, fed *ad libitum*, and cages are changed 2-3 times weekly. Wt or stable expression
103 of the ARL13B transgene conjugated to enhanced green fluorescent protein (*Arl13B-EGFP^tg*) in
104 the genome of a founder C57BL/6 mouse were used. Importantly, *Arl13B-EGFP^tg* mice do not
105 have a distinct behavioral or anatomical phenotype from C57BL/6 mice[38,45]. Hippocampi were
106 dissected from P0-P1 mice (n= 6-8 pups per experiment) under a scope in a cold solution Hank's
107 Balanced Salt Solution (HBSS, 14185-052, Gibco) containing HEPES (100 mM) (15630-080,
108 Gibco) and digested in Trypsin 0.025% (25-050-CI, Corning) at 37°C for 5 minutes. Solution was
109 removed and the tissue were gently triturated using a P1000 in 1 mL of platting media which
110 consisted of Neurobasal A (10888-022, Gibco) containing B27 supplement (17504044, Gibco), 1
111 % penicillin/streptomycin (15140148, Gibco), 10 % normal horse serum (NHS, 260500, Gibco),
112 1% glucose (A2494001, Gibco) and GlutaMAX (350500-061, Gibco). Cells were seeded only in
113 the glassed surface area of the dish/coverslip using platting media at 1 x 10^6 cells/dish or
114 coverslip. Glass bottom dishes (P35G-1.0-14-C, Mattek) or coverslips were coated only on the
115 glassed surface area using Matrigel (1:20, 356234, Corning). Media was replaced with a feeding
116 medium (media without NHS) after 3 hours of seeding. After 1-3 days in culture, WT hippocampal
117 neuron cultures were infected with lentivirus vector encoding for cilia reporters and sensors (See

118   section 2.3). All hippocampal neurons (WT or *Arl13B-EGFP[tg]*) were cultured for up to 14 days and
119   the feeding medium was changed every 2-3 days.
120
121   *2.2 Electrophysiology*
122   Below are described strategies for measuring ciliary ion channels from cells expressing
123   cilia-specific fluorescent proteins with "on-cilia" patch clamp configuration (**Figure 1A**). This
124   method is an extension of the voltage clamp method established more than 50 years ago with
125   details optimized for cilia membrane ion channel recordings[6,41,43]. Electrophysiology experiments
126   were performed using either an inverted confocal or widefield microscope (**Table 3**). We used a
127   20x objective lens to locate cells projecting the primary cilium above the focal plane or to the side
128   of the cell, and having sufficient fluorescence, then switched to a 60x water emersion objective
129   with a 2x photomultiplier to visualize the cilia during seal formation. To capture images and video
130   recordings of the cilia patch configuration, a standard CCD or CMOS camera on a widefield
131   microscope sufficient.
132
133   *2.2.1 Glass electrode fabrication*
134   Filamented glass with inner and outer diameters of 0.84 and 1.4 mm, respectively were
135   used. The resistance of the "pulled" electrodes manufactured using a laser-heated puller were
136   between 5-9 MΩ with an inner aperture of 0.5-1 µm in diameter. These electrodes were then
137   polished using a commercially available electrode polisher (**Table 3**). This step smoothens the
138   surface of the glass and narrows the aperture of the tip of the electrode, thereby increasing the
139   resistance of electrode. To determine the optimal pipette resistance for the cilia recording, the
140   resistance capable of achieving a high resistance seal within the cilia membrane (>10 GΩ) were
141   correlated from many attempts. Afterwards, we used a scanning electron microscope to measure
142   the inner diameter of each patch electrode used.
143
144   *2.2.2 Single channel recordings*
145   Single channel currents were measured from the primary cilia membrane an Axon 200B
146   (Molecular Devices) amplifier connected to Digitdata 1550 digitizer (**Table 3**), as previously
147   described[6,41]. The standard pipette solution contained (in mM): 100 NaCl, 10 HEPES, pH 7.4 with
148   NaOH and adjusted to 300-305 mOsm/L with mannitol. High potassium bath solutions containing
149   130 KCl, 15 NaCl, 10 HEPES, 1.8 $CaCl_2$, 1 $MgCl_2$, pH 7.4 with KOH and 300-305 mOsm/L, were
150   used to neutralize the membrane potential. Of note, the composition of the saline which
151   determines the ion to be used as a charge carrier depends on the type of ciliary ion channel
152   opening events to be tested. To measure the PKD2L1 channels activity on the neuronal cilia
153   membrane, as exampled here, the pipette solution contained (in mM): 100 $CaCl_2$, 10 HEPES, pH
154   7.4 with $Ca(OH)_2$ and adjusted to 300-305 mOsm/L with mannitol. The permeability of monovalent
155   cations (P_{X+}/P_{Na}) can be determined by observing the shift in reversal potential when the external
156   Na^+ bath solution is replaced. Recording saline was front filled and backfilled into these pipettes
157   to ensure electrical continuity. Data was collected using an Axopatch 200B patch clamp amplifier
158   and the pClamp 10 software (Molecular Devices, **Table 3**). As a rule of thumb, we recommend
159   sampling the current 5x more frequently (25 KHz) than the low-pass Bessel filter rate. While this

160   makes the size of the acquisition file larger, these settings allow for the sufficient sampling of both
161   single and whole cilia currents, which can be re-sampled during the analysis phase.
162
163   *2.3 Cilia-targeted identification reporters, Ca^{2+} sensors and cAMP sensors*
164   Cilia-targeted identification reporters (ARL13B-EGFP; ARL13B-mCherry); Ca^{2+} sensors
165   (ARL13B-GFP-RGECO1; 5-HT6R-RGECO1) were custom synthesized (VectorBuilder) into the
166   lentiviral cassettes (pLV[Exp]-puro-CMV) to generate lentivirus (10^8 titer) solutions encoding for
167   each reporter or sensor. Primary hippocampal neurons isolated from WT or ARL13B-EGFP^{tg} mice
168   were transduced overnight at DIV 2-3 (MOI=1-2) in a solution containing feeding media and
169   polybrene (4 μg/mL). Experiments we carried out from 3 days after transduction. For the cAMP
170   sensor coupled to the 5-HT6R encoded by the BacMam vector (cilia-targeted cADDis sensor,
171   D0201G, Montana Molecular), cultured neurons from WT mice were used and transduced
172   overnight at DIV 5 according to the manufacturer instruction. Fluorescent intensity of the cADDis
173   (Green) decreases in response to increases in cAMP. Experiments we conducted from 1 day after
174   transduction. When both 5-HT6R-RGECO1 and 5HT6R-cADDis sensors were evaluated
175   together, cells were transduced as mentioned above with cADDis transduction performed one
176   day prior to the experiments. Ciliated neurons were filmed (1 frame/sec) before and after the
177   application of different solutions: To calibrate the ARL13B-GFP-RGECO1 sensor, different
178   calcium concentrations (0, 1, 10 or 100 μM) in the presence of ionomycin (1 μM) were applied.
179   Bath standard solution was composed by (in mM): 140 NaCl, 10 HEPES, 5 KCl, or otherwise
180   stated, and pH 7.4 was adjusted with NaOH. Ratiometric fluorescence intensity was calculated by
181   the ratio of RGEGO1/GFP and normalized by the fluorescence average of the initial 30 sec of
182   filming. For the 5-HT6R-RGECO1 sensor alone, solutions containing ionomycin alone (1 μM) or
183   with calcium (10 μM) were assessed. For the cADDis alone, the 5-HT6R agonist WAY 181187 (1
184   μM) or in a combination with the 5-HT6R antagonist SB 271046 (100 μM, pre-incubation for 10
185   minutes) was tested. When neurons were transduced with both 5-HT6R-RGECO1 and cADDis,
186   WAY 181187 followed by ionomycin (1 μM) + Ca^{2+} (10 μM) were applied. Fluorescence intensity
187   was calculated by the ratio of RGEGO1 (red)/GFP (green) and normalized by the fluorescence
188   average of the initial 30 sec of filming, or by the ΔF/F0 in which F0 is the fluorescence average of
189   the initial 30 sec of filming.
190
191   *2.4 Drugs and salts*
192   Salts used to prepare bath solutions are manufactured by Sigma Aldrich (St. Louis, MO)
193   or Fisher (Waltham, MA). Ionomycin free acid (ref # 407950, Millipore Sigma), WAY 181187
194   oxalate (ref # 5589, Tocris Biosciences, UK), SB 271046 hydrochloride (ref #3368, Tocris
195   Biosciences, UK) and thapsigargin (ref # T7458, ThermoFisher) were initially dissolved in DMSO
196   (ref # D2650, Sigma Aldrich) and diluted in working solutions according to each experiment. α-
197   hemolysin (ref #H9395, Sigma Aldrich) was dissolved in water (stock solution of 0.5 mg/mL).
198
199   *2.5 Data analysis*
200   Electrophysiology data was analyzed with ClampFit (Molecular Devices) and IGOR Pro
201   (Wavemetrics) software. Data collected with the sensors were evaluated for normality using
202   Anderson-Darling test. For Arl13B-GFP-RGECO1 ratiometric experiments, one-way ANOVA

203 followed by Holm-Sidak's multiple comparisons test were used to analyze the data of peak
204 intensity. For the 5-HT6R-RGECO1 experiments, multiple paired t-tests were used.
205
206 **3 Results**
207
208 *3.1 Neuronal primary cilia electrophysiology*
209 Glass electrodes with submicron aperture are fabricated to establish high resistance seals with
210 the primary cilia membrane to measure stochastic single channel open events ("on-cilia"
211 configuration) or total ciliary current ("whole-cilia" configuration)[40,41]. After forming giga-ohm
212 resistance seals, the neuronal cilia can be severed ("inside-out" configuration) from the soma to
213 access and apply effectors to the internal side of the cilia membrane (**Figure 1A-F**)[41]. The primary
214 cilium is electrically insulated from the cell body, with its own resting membrane potential (-17 mV)
215 and Ca^{2+} calcium concentration (350-700 nM)[36,37,41]. To match the geometry of the neuronal
216 primary cilia, microelectrodes are fabricated in two steps. First, long taper borosilicate electrodes
217 with 900-600 nm tip diameters are created using a heated filament or laser glass puller. Second,
218 the electrode tip is polished using a microforge so that the lumen approximates the diameter
219 (~350 nm) of the primary cilia (**Figure 1B, E**). Neuronal primary cilia can be visualized using
220 brightfield microscopy, but to faithfully distinguish these structures from filipodia, we used
221 genetically encoded fluorescent ciliary markers (**Table 2**). Here, the cilia specific proteins such
222 ARL13B are conjugated with fluorescent protein and expressed as a transgene in the mouse
223 genome (ARL13B-EGFP[tg]) or transduced virally in cultures of neonatal hippocampal neurons
224 (ARL13B-GFP or ARL13B-mCherry). We observed that cultured for 6-10 days offered the highest
225 number of ciliated neurons for our electrophysiology experiments (**Supplemental Figure 1**). We
226 recommend selecting neurons with primary cilia projecting above the soma's focal plane and
227 towards the recording electrodes path of approach. The electrodes approach and course position
228 of the ciliated neurons can be achieved with lower magnification (20-40x objective). However,
229 once the recording electrode approaches 100 μm from the cilia, the objective magnification should
230 be increased (60-100x water or oil) which have limited working distances. Turning off the
231 fluorescent light source to minimize photobleaching of the cilium. Typical gear-driven
232 manipulators can be used to patch primary cilia, but we recommend using piezo manipulators
233 which have minimal drift (**Table 3**). Inward suction (2-10 mmHg) the tip of the cilia membrane
234 seals onto the pipette electrode tip, creating electrical resistance (R_{cilia}) greater than 10 GΩ. We
235 have determined that electrodes with 280-410 nm inner diameter and resistance of 17-32 MΩ
236 frequently achieved high resistance seals of ciliary membranes allowing the recording of channels
237 activity (**Figure 1F-J**). Exemplar PKD2L1 single channel open events recorded from a
238 hippocampal primary cilium in the "on-cilia" configuration are shown in **Figure 1K**. Importantly,
239 the command potential and the current directionality are reported in the opposite polarity and
240 inverted directionality in the "on-cilia" configuration, to be consistent with conventions for reporting
241 electrophysiology data sets. Single channel open probability can be reliably determined over a
242 series of 1-5 second epochs and respective unitary conductance can be estimated by fitting the
243 average current magnitude over applied membrane potentials to fit a linear equation.
244
245 *3.2 Calcium sensor Arl13B-GFP-RGECO1 in hippocampal neurons.*

246   Primary cilia have 5-fold higher resting Ca^{2+} concentration and contain calcium-binding
247   proteins with high disassociation constants which are frequently impacted by genetic variants
248   implicated in neuronal ciliopathies[36,37]. Because they are resistant to chemical loading by dye
249   indicators, native neuronal cilia proteins (Smo, ARL13B, 5-HTR6) can be linked to calcium sensor
250   fluorescent reporters (GCaMP, GECO). An additional non-calcium dependent fluorescent reporter
251   (mCherry, EGFP) can be added to the sensor to normalize the Ca^{2+} fluorescence response and
252   provide ratiometric measurements which allow quantification of free Ca^{2+} concentration within the
253   primary cilia. For expression in neonatal hippocampal neuron cilia, we linked ARL13B-GFP with
254   red-shifted RGECO1 (genetically encoded Ca^{2+} indicator for optical imaging) within a lentivirus
255   expression vector. After 5-7 days in culture, murine hippocampal neurons become electrically
256   excitable, generating spontaneous action potentials when assessed by current clamp[44]. At this
257   time point, spontaneous primary cilia calcium dynamics are captured by the ARL13B-GFP-
258   RGECO1 sensor transduced hippocampal neurons (**Figure 2A**). Thess endogenous calcium
259   waves can be visualized in real time (1 frame/sec) using a three-dimensional structured
260   illumination microscopy (3D-SIM) in standard solution containing 1.8 mM calcium, **Supplemental
261   Video 1**). To minimize potential biases associated with external calcium transients, we conducted
262   our experiments using a calcium-free standard bath solution, in which spontaneous calcium
263   waves in the neuronal primary cilia were markedly diminished (**Figure 2B**). After exchanging
264   external conditions in the presence of the Ca^{2+} ionophore ionomycin, we observed external Ca^{2+}
265   dose-dependent (1-100 μM) increases in RGECO1 fluorescence intensity (**Figure 3A,
266   Supplemental Video 2**). Ionomycin alone (no external Ca^{2+}) increased cilia Ca^{2+}-dependent
267   fluorescence, suggesting that the ionophore is stimulating release of intracellular store Ca^{2+},
268   which propagates into this cilia organelle compartment. Although not significant, when ionomycin
269   was combined with 1 μM Ca^{2+}, it was less effective at stimulating cilia RGECO responses
270   compared to ionomycin alone. We speculate that ionomycin efficacy in triggering intracellular Ca^{2+}
271   store release was impacted by its 1:1 binding ratio to free external calcium[45]. To verify whether
272   intracellular calcium released from cytoplasmic stores was entering the primary cilia, we re-
273   analyzed the data with ROIs on both base and tip of the cilia. In every neuron tested, ionomycin-
274   induced calcium responses initiated from the cytoplasm and propagated to the primary cilium
275   (**Supplemental Figures 2A, B**). In addition, we repeated the experiment but first applied
276   thapsigargin (SERCA pump inhibitor) for depletion of ER Ca^{2+} stores of the neurons for 3 minutes.
277   We observed that thapsigargin triggered a mild increase in cilia Ca^{2+}, but an attenuated cilia Ca^{2+}
278   response from externally applied ionomycin (**Supplemental Figure 2C**). These observations
279   demonstrate the new primary cilia Ca^{2+} sensors sensitivity to external and store operated calcium
280   signaling in hippocampal neurons. Moreover, the sensor also detected calcium transients under
281   micromolar concentrations of external calcium (500 nM) after permeabilization with alpha
282   hemolysin (10 μg/mL) for 3 minutes (**Supplemental Figure 2D**). Thus, the use of calcium-sensors
283   such as ARL13B-GFP-RGECO1, can be deployed to further examine the relationship between
284   store operated Ca^{2+} signals and neuronal primary cilia responses in the central nervous system.
285
286   *3.3 Cilia-targeted Ca^{2+} and cAMP sensors coupled to the 5-HT6R in neurons.*
287   Hippocampal neuron primary cilia extend from the soma and form serotonergic synapses
288   with axons that house GPCR effort that control the epigenetic signaling[15]. Common

289 polymorphisms in serotonin receptor type 6 (5-HTR6) are associated with early onset of
290 Alzheimer's disease, development of schizophrenia and bipolar disorders, suggesting their role
291 in cognition, learning, and mood regulation[18,21,46,47]. 5-HT6R is highly expressed brain regions like
292 the hippocampus, cortex, and basal ganglia[18] but these receptors almost exclusively traffic to the
293 primary cilia of neurons. 5-HT6R is a GPCRs coupled to Gαs pathway that activates adenylyl
294 cyclase which catalyzes production of cAMP from ATP, but it may also stimulate a non-canonical
295 Gαq$_{/11}$-Rho pathway in cilium-axon synapse[15]. To assess local [Ca^{2+}] and [cAMP] changes in
296 primary cilia using the same cilia-targeted moiety, we coupled 5-HT6R to RGECO1 (5-HT6R-
297 RGECO1) within a lentivector and compared these results with the commercially available
298 BacMan 5-HT6R-cADDi cilia cAMP sensor (**Table 2**). Like the ARL13B-GFP-RGECO1 sensor,
299 validation experiments of the 5-HT6R-RGECO1 sensor demonstrates Ca^{2+}-dependent sensitivity
300 after permeabilized by ionomycin (**Figure 4A, B, Supplemental Video 3**). We used a
301 pharmacological approach to validate the 5-HT6R-cADD primary cilia cAMP sensor. Here, cAMP-
302 dependent fluorescence increased upon WAY 181187 (5-HT6R agonist) application, but this
303 effect was ablated when neurons were incubated with the 5-HT6R antagonist, SB 271046 (**Figure
304 4C, D, Supplemental Figure 3**). To simultaneously assess [Ca^{2+}] and [cAMP] changes within the
305 primary cilia, we co-expressed 5-HT6R-RGECO1 with 5-HT6R-cADDis in the cultured primary
306 hippocampal neurons (**Figure 4, Supplemental Video 4**). Stimulation of cAMP production by
307 WAY 181187 was detected by the 5-HT6R-cADDis sensor, whereas the Ca^{2+}-dependent 5-HT6R-
308 RGECO1 fluorescence response remained unchanged. However, Ca^{2+} permeabilization by
309 ionomycin only enhanced the 5-HT6R-RGECO1 fluorescence, whereas the signal from the cAMP
310 sensor remained unchanged. These observations demonstrate the fidelity of using these probes
311 in reporting unambiguous fluorescence levels proportional to [cAMP] and [Ca^{2+}] measured within
312 the same primary cilia compartment. In addition, our results indicate primary cilia [Ca^{2+}] and
313 GPCR-mediated [cAMP] dynamics are not interdependent, a finding which delineates this
314 organelle's localized signaling from the Ca^{2+}-cAMP interplay reported globally the soma[48]. Clearly,
315 these findings highlight the importance of using the cilia-specific sensors described when testing
316 signal transduction pathways within this privileged organelle.
317

4. SUMMARY

319 We have described in detail methodologies and validation of fluorescence sensors for the
320 detection cAMP and Ca^{2+} within hippocampal neuronal primary cilia. Previous work has reported
321 the use of similar sensors in fibroblast, epithelial and pancreatic beta immortalized cell lines
322 (**Table 1**)[36-38,49]. Thus to our knowledge, this is the first methods report of their use in primary
323 hippocampal neurons. In addition we have provided details of the electrophysiology approach for
324 directly recording PKD2L1 in the primary cilia— a Ca^{2+} channel which regulates hippocampal
325 interneuron excitability[6]. It is expected that neuronal primary cilia also express other ion channels
326 that conduct monovalent cations (K$^+$) and anions (Cl$^-$) to maintain its ionic homeostasis and the
327 organelles resting membrane potential. Thus, the described primary cilia patch clamp method can
328 be used to define other cilia ion channel properties. Although not presented here, the Ca^{2+} or
329 cAMP sensors could be combined with electrophysiology to assess the impact of GPCR
330 modulation of channel function. Recent work has expanded the tools available to include light-
331 activated GPCRs to assess neuronal cilia regulation of behavior in vivo[50] and nanobody-directed

332 targeting of optogenetic tools to control cAMP levels in the primary cilium[51,52]. Take together these
333 expanding methodologies and experimental approaches can be used to uncover underlying
334 molecular dysfunction and signaling that cause neuronal ciliopathies; electrochemical signaling
335 across the axo-ciliary synapse; and illuminate the basic biology of primary cilium.
336

343 **Materials availability statement.**

344 All mammalian cell expression constructs used in this study are available without restriction upon
345 written request to the corresponding author or otherwise will be made available through Addgene
346 (https://www.addgene.org/).

347

348 **Conflict of Interest Statement**
349 Authors have no conflict of interest.
350

351 **Data Availability Statement**
352 Primary data sets and analysis are archived through Northwestern University Institutional
353 Repository (ARCH) and will be made available upon publication of this manuscript (DOI:
354 https://doi.org/10.21985/n2-s825-ay98).
355

356 **FIGURE LEGENDS**
357

358 **Figure 1: Neuronal primary cilia electrophysiology.** We used the "on-cilia" patch clamp
359 configuration with equivalency circuit as represented (**A**). Hippocampi was dissected from P0
360 mice expressing cilia-specific fluorescent protein (Arl13B-EGFP[tg] mice) and cells were seeded in
361 glass bottom dishes. Ciliated neurons were patched (DIV 6-10) using the whole cell (**B-E**) or cilia
362 patch clamp (**F-I**) configurations. Scanning electron microscope images of a whole-cell (**B**) and
363 cilia patch (**F**) electrodes were taken for comparison purposes between the two techniques. The
364 correlation between electrode resistance versus its lumen diameter with successful giga-seal
365 formation (blue circles indicate successful trials) is represented in Figure 1J. The current traces
366 of PKD2L1 channels present in the cilium are represented in Figure 1K. Scale bar for E, I: 10 µm.
367

368 **Figure 2: Spontaneous Ca^{2+} waves in the neuronal primary cilia.** On DIV 2-3, hippocampal
369 WT cultured cells were transduced overnight with the lentivector ARL13B-GFP-RGECO1 (MOI=
370 1-2) and 5 days after transduction, ratiometric experiments were performed under a confocal
371 microscope. Neurons were imaged in the standard solution containing 1.8 mM of calcium (**A**) or
372 in the standard solution (calcium-free) (**B**). Fluorescence intensity was calculated by the ratio of

373   RGEGO1 (red)/GFP (green) and normalized by the fluorescence average of the initial 10 sec of

374   filming, or when cells fluorescence returned to the baseline levels.

375

376   **Figure 3: The cilia targeted calcium sensor ARL13B-GFP-RGECO1.** On DIV 2-3, hippocampal

377   cultured cells were transduced overnight with the lentivector Arl13B-GFP-RGECO1 (MOI= 1-2)

378   and 5 days after transduction, ratiometric experiments were performed under a confocal

379   microscope. Ciliated neurons were then filmed (1 frame/sec) before and after the application of

380   solutions containing different calcium concentrations (0, 1, 10 or 100 µM) in the presence of

381   ionomycin (1 µM). Fluorescence intensity was calculated by the ratio of RGEGO1 (red)/GFP

382   (green) and normalized by the fluorescence average of the initial 30 sec of filming. (**A**) The time

383   course of fluorescence intensity before and after solutions application. (**B**) The peak of

384   fluorescence intensity of each solution evaluated. One-way ANOVA followed by Holm-Sidak's

385   multiple comparisons test was performed. p values are described in the figure (**C**) Representation

386   of the ciliated neurons chosen for the experiment and the fluorescence course before and after

387   each calcium solutions application. Scale bar: 10 µm.

388

389   **Figure 4: Combining primary cilia sensors for simultaneous Ca^{2+} and cAMP**

390   **measurements.** 5-HT6R-RGECO1 alone or in combination with the cilia cAMP sensor 5-HT6R-

391   cADDis. Hippocampi was dissected from P0 Arl13B-EGFP[tg] (**A, B**) or WT (**C-F**) mice and cells

392   were seeded in glass bottom dishes. On DIV 2-3, hippocampal cultured cells were transduced

393   overnight with the lentivector 5-HT6R-RGECO1 (MOI= 1-2) and 5 days after transduction,

394   ratiometric experiments were performed under a confocal microscope. For the 5-HT6R-cADDis,

395   cells were transduced one day before the experiments. Ciliated neurons were then filmed (1

396   frame/sec) before and after the application of solutions containing ionomycin alone (1 µM) (n= 9)

397   or with calcium (10 µM) (n= 9) (**B**), 5-HT6R agonist WAY 181187 (1 µM) (n= 5) (**D**), or with both

398   WAY 181187 (1 µM) followed by ionomycin (1 µM) + Ca^{2+} (10 µM) (n= 13) (F). Fluorescence

399   intensity was calculated by the ratio of RGEGO1 (red)/GFP (green) and normalized by the F0

400   (fluorescence average of the initial 30 sec of filming) (**B**) or by the ∆F/F0 (**D, F**). Scale bar: 10 µm.

401   Unpaired t test for B, * p< 0.05.

402

403

404

405

406

407

408

409

410

411   **Table 1: Neuronal ciliopathy syndromes.** A tabulated list of neuronal ciliopathies with their

412   associated genetic variants and clinical pathology. Note some neuronal ciliopathies have different

413   diagnoses but are associated with variants that impact the same gene. Renal abnormalities

414   comorbid with neuronal ciliopathies most frequently manifest as early onset polycystic kidney

415   disease.

416

Syndrome (*Gene variants associated*)	Pathology
Joubert syndrome (*CEP290; TMEM67; AHI1; CC2D2A; INPP5E; ARL13B; RPGRIP1L; KIF7; TCTN1-3; MKS1; TMEM216*)	Characterized by abnormal brain development, leading to motor and cognitive impairment.
Bardet-Biedl syndrome (*BBS1-18 includes MSKKS, LZTFL1, SDCCAG8 and ARL6; IFT27*)	This multisystem disorder often involves cognitive impairment, obesity, and vision loss due to retinal degeneration.
Meckel-Gruber syndrome (*MKS1; TMEM67; CC2D2A; TMEM216; CEP290; B9D1; TMEM231; RPGRIP1L ; TCTN1-3; TMEM107; NPHP3*)	A severe disorder that often leads to brain malformations and is usually lethal early in life.
Alström syndrome (*KIF7; WDR35; DYNC2H1; IFT80; MKS1*)	A condition that can cause vision and hearing loss, obesity, and heart failure, along with neurological symptoms.

417

418 **Table 2. A primary cilia toolbox.** Genetically encoded fluorescent reporters for identification,
419 Ca^{2+} concentration and GPCR signaling within primary cilia. Previously published expression
420 constructs or transgenic animal models are listed with corresponding citations.

421

Cilia identification reporters
Arl13b-EGFP[tg] (transgenic mouse)[41]
ARL13B-mCherry (lentiviral vector) *This manuscript.*
ARL13B-EGFP (lentiviral vector), *This manuscript.*
Cilia cAMP signaling sensors, modulators
5HT6R-cADDi (cAMP, BacMam vector, Montana Molecular)[38]
bPAC, LAPD, mlCNBD-FRET (light activated cAMP modulators)[51]
Cilia [Ca²⁺] sensors
Smo-mCherry-GCaMP3 (mammalian expression vector)[37]
Smo-mCherry-GECO1 (mammalian expression vector)[37]
ARL13B-GFP-RGECO1 (lentiviral vector), *This manuscript.*
5HT6R-GECO[36]
5HT6R-RGECO1 (lentiviral vector) *This manuscript.*

422
423

424

425

426

427

428 **Table 3. List of equipment used with manufacture part numbers.**

COMPONENT	PART NUMBER, MODEL	MANUFACTURE
Bright field microscope components		
Equipped with standard components	IX73	Olympus

Objective 20x, Air U Plan Fluorite, NA 0.5, WD 1.6 mm	1-U2B525	Olympus
Objective 40x, Air U Plan Fluorite, NA 0.75, WD 0.51 mm	1-U2B527	Olympus
Objective 60x, water emersion NA 1.2, WD 0.51 mm	UPLSAPO	Olympus
Fluorescent light source	Lumen 200	Prior
Filter for EGFP, GCaMP3, mEmerald 470/20x, 485DM, 517/45m	U-FGFP BX3 GFP/BLUE WIDE	Olympus
Filter for EYFP, Venus, Citrine 495/10x, 505DM, 537/45m	U-FYFP; BX3 YFP/YELLOW NARROW	Olympus
Filter for RFP, mCherry, DsRED 545/20x, 565DM, 597/55m	U-FRFP; BX3 RFP/GREEN WIDE	Olympus
Electrophysiology and imaging components		
Patch clamp amplifier	Axopatch 200B	Molecular Devices
Digital to analogue signal converter	Digidata 1440	Molecular Devices
CMOS camera	ORCA-FLASH 4.0LT	Hamamatsu
CCD camera	U-TV1X-2-7	Olympus
Rapid perfusion system	VC-77CS "Fast step system"	Warner Instruments
High speed pressure clamp system	HSPC-1	ALA Scientific Instruments
Dual micromanipulator System (Stepper motor driven)	MP-300	Sutter Instruments
Dual micromanipulator System (Linear piezo driven)	Inchworm, uM 3-axis System 69-3432	Sensapex
Microelectrode fabrication components		
Flaming brown filament type micropipette electrode puller	P-97 3 mm box filament Settings: Heat = ramp test value; Pull = 44; Velocity = 65; Delay= 200; Pressure = 600	Sutter Instruments
Laser-Based micropipette electrode puller	P-2000	Sutter Instruments
Capillary glass O.D. 1.5 mm, I.D. 0.84 mm	1B150F-4	World Precision Instruments

429

430

Supplemental Figure 1: Cultures of ciliated neonatal hippocampal neurons. Hippocampi were dissected from P0 mice (n= 6-8), dissociated, cell-strained and cells were seeded in glass bottom dishes ($1x10^5$ cells/dish). Images were taken under a light microscope (40x) close to the border of the glass where the density of cells are not too high and allows better visualization of the primary cilia within time. (**A**) Cells after 4 h of seeding, (**B**) DIV 1, (**C**) DIV 6, and (**D**) DIV 9.

(**E, F**) Cultured hippocampal neurons at DIV 6 after infection with lentivirus for primary cilia identity reporters ARL13B-EGFP or ARL13B-mCherry.

Supplemental Figure 2: Ionomycin favors Ca^{2+} influx of from the cytoplasm to the primary cilia by releasing calcium from cytoplasmatic compartments. On DIV 2-3, hippocampal WT cultured cells were transduced overnight with the lentivector ARL13B-GFP-RGECO1 (MOI= 1-2) and 5 days after transduction, ratiometric experiments were performed under a confocal microscope. Ciliated neurons were then filmed (1 frame/sec) before and after the application of ionomycin alone (1 µM) (**A**) or in a combination with Ca^{2+} (10 µM) (**B**). ROIs were placed on both base and tip of the cilia. To verify the role of stored calcium in the influx to the primary cilia, thapsigargin (Thapsi, 2 µM, blue, n= 5) or DMSO (control, red, n= 5) treatments were performed for 3 min followed by the application of ionomycin together with Ca^{2+} 10 µM. Interestingly, we observed a small increase in calcium influx in the cilia seconds after thapsigargin application. After 3 min, the sensor response to ionomycin together with Ca^{2+} 10 µM in the cilia was smaller when compared to control group (DMSO) (**C**). When cells were permeabilized with α-hemolysin (α-HL, 10 µg/mL) for 3 min, the sensor also detected calcium changes in the primary cilia upon external application of 500 nM calcium (n= 9). Ionomycin 1 µM was used as control (n= 6) (D). Fluorescence intensity was calculated by the ratio of RGEGO1 (red)/GFP (green) and normalized by the fluorescence average of the initial 30 sec of filming.

Supplemental Figure 3: Specificity of cAMP sensor when expressed in neuronal primary cilia. On DIV 5, hippocampal WT cultured cells were transduced overnight with 5-HT6R-cADDis and 1 day after transduction, fluorescence experiments were performed under a confocal microscope. Ciliated neurons were then filmed (1 frame/sec) after the pre-incubation with SB 271046 (100 µM, n= 5) or DMSO (control, n=5) followed by the 5-HT6R agonist WAY 181187 (**A**). To confirm receptor specificity to the primary cilia 5-HT6R, we applied WAY 181187 followed by forskolin (100 µM, an activator of adenylyl cyclase) on the neurons pre-incubated with SB 271046 (100 µM) (n= 3) (**B**). To understand if cAMP production was coming from the cytoplasmic 5-HT6R rather than ciliary 5-HT6R, ROIs were placed on both base and tip of each cilium analyzed. As can be observed, cAMP production induced by WAY 181187 was homogeneous on both base and tip, indicating that cAMP is being produced within the primary cilia (**C**).

Supplemental Video 1. Primary cilia endogenous Ca^{2+} waves.

Supplemental Video 2. Primary cilia ratiometric Ca^{2+} sensor (ARL13B-GFP-RGECO1) responses to ionomycin with Ca^{2+} 100 µM.

Supplemental Video 3. Primary cilia Ca^{2+} sensor (5-HT6R-RGECO1) responses to ionomycin with Ca^{2+} 10 µM.

Supplemental Video 4. Fluorescence responses from cAMP (5-HT6R-cADDis) and Ca^{2+} (5-HT6R-RGECO1) sensors co-expressed in hippocampal primary cilia.

479

REFERENCES

481

1. Pazour, G. J. & Witman, G. B. The vertebrate primary cilium is a sensory organelle. *Curr Opin Cell Biol* **15**, 105-110, doi:10.1016/s0955-0674(02)00012-1 (2003)

2. Jurisch-Yaksi, N., Wachten, D. & Gopalakrishnan, J. The neuronal cilium - a highly diverse and dynamic organelle involved in sensory detection and neuromodulation. *Trends Neurosci* **47**, 383-394, doi:10.1016/j.tins.2024.03.004 (2024)

3. Gopalakrishnan, J. *et al.* Emerging principles of primary cilia dynamics in controlling tissue organization and function. *EMBO J* **42**, e113891, doi:10.15252/embj.2023113891 (2023)PMC10620770.

4. Plotnikova, O. V., Pugacheva, E. N. & Golemis, E. A. Primary cilia and the cell cycle. *Methods Cell Biol* **94**, 137-160, doi:10.1016/S0091-679X(08)94007-3 (2009)PMC2852269.

5. Macarelli, V., Leventea, E. & Merkle, F. T. Regulation of the length of neuronal primary cilia and its potential effects on signalling. *Trends Cell Biol* **33**, 979-990, doi:10.1016/j.tcb.2023.05.005 (2023)PMC7615206.

6. Vien, T. N., Ta, M. C., Kimura, L. F., Onay, T. & DeCaen, P. G. Primary cilia TRP channel regulates hippocampal excitability. *Proc Natl Acad Sci U S A* **120**, e2219686120, doi:10.1073/pnas.2219686120 (2023)PMC10235993.

7. Ott, C. M. *et al.* Ultrastructural differences impact cilia shape and external exposure across cell classes in the visual cortex. *Curr Biol* **34**, 2418-2433 e2414, doi:10.1016/j.cub.2024.04.043 (2024)PMC11217952.

8. Wu, J. Y. *et al.* Mapping of neuronal and glial primary cilia contactome and connectome in the human cerebral cortex. *Neuron* **112**, 41-55 e43, doi:10.1016/j.neuron.2023.09.032 (2024)PMC10841524.

9. Klink, B. U., Gatsogiannis, C., Hofnagel, O., Wittinghofer, A. & Raunser, S. Structure of the human BBSome core complex. *Elife* **9**, doi:10.7554/eLife.53910 (2020)PMC7018512.

10. Tian, X., Zhao, H. & Zhou, J. Organization, functions, and mechanisms of the BBSome in development, ciliopathies, and beyond. *Elife* **12**, doi:10.7554/eLife.87623 (2023)PMC10356136.

11. Bangs, F. & Anderson, K. V. Primary Cilia and Mammalian Hedgehog Signaling. *Cold Spring Harb Perspect Biol* **9**, doi:10.1101/cshperspect.a028175 (2017)PMC5411695.

12. Niehrs, C., Da Silva, F. & Seidl, C. Cilia as Wnt signaling organelles. *Trends Cell Biol*, doi:10.1016/j.tcb.2024.04.001 (2024)

13. Breunig, J. J. *et al.* Primary cilia regulate hippocampal neurogenesis by mediating sonic hedgehog signaling. *Proc Natl Acad Sci U S A* **105**, 13127-13132, doi:10.1073/pnas.0804558105 (2008)PMC2529104.

14. Park, S. M., Jang, H. J. & Lee, J. H. Roles of Primary Cilia in the Developing Brain. *Front Cell Neurosci* **13**, 218, doi:10.3389/fncel.2019.00218 (2019)PMC6527876.

15. Sheu, S. H. *et al.* A serotonergic axon-cilium synapse drives nuclear signaling to alter chromatin accessibility. *Cell* **185**, 3390-3407 e3318, doi:10.1016/j.cell.2022.07.026 (2022)PMC9789380.

16. Schulz, S., Handel, M., Schreff, M., Schmidt, H. & Hollt, V. Localization of five somatostatin receptors in the rat central nervous system using subtype-specific antibodies. *J Physiol Paris* **94**, 259-264, doi:10.1016/s0928-4257(00)00212-6 (2000)

17. Cone, R. D. Anatomy and regulation of the central melanocortin system. *Nat Neurosci* **8**, 571-578, doi:10.1038/nn1455 (2005)

524 18 Dupuy, V. *et al.* Spatiotemporal dynamics of 5-HT(6) receptor ciliary localization during mouse
525   brain development. *Neurobiol Dis* **176**, 105949, doi:10.1016/j.nbd.2022.105949 (2023)
526 19 Barbeito, P. & Garcia-Gonzalo, F. R. HTR6 and SSTR3 targeting to primary cilia. *Biochem Soc*
527   *Trans* **49**, 79-91, doi:10.1042/BST20191005 (2021)
528 20 Siljee, J. E. *et al.* Subcellular localization of MC4R with ADCY3 at neuronal primary cilia underlies
529   a common pathway for genetic predisposition to obesity. *Nat Genet* **50**, 180-185,
530   doi:10.1038/s41588-017-0020-9 (2018)PMC5805646.
531 21 Wachten, D. & Mick, D. U. Signal transduction in primary cilia - analyzing and manipulating GPCR
532   and second messenger signaling. *Pharmacol Ther* **224**, 107836,
533   doi:10.1016/j.pharmthera.2021.107836 (2021)
534 22 Handel, M. *et al.* Selective targeting of somatostatin receptor 3 to neuronal cilia. *Neuroscience*
535   **89**, 909-926, doi:10.1016/s0306-4522(98)00354-6 (1999)
536 23 Lee, J. E. & Gleeson, J. G. Cilia in the nervous system: linking cilia function and
537   neurodevelopmental disorders. *Curr Opin Neurol* **24**, 98-105,
538   doi:10.1097/WCO.0b013e3283444d05 (2011)PMC3984876.
539 24 Valente, E. M., Rosti, R. O., Gibbs, E. & Gleeson, J. G. Primary cilia in neurodevelopmental
540   disorders. *Nat Rev Neurol* **10**, 27-36, doi:10.1038/nrneurol.2013.247 (2014)PMC3989897.
541 25 Mill, P., Christensen, S. T. & Pedersen, L. B. Primary cilia as dynamic and diverse signalling hubs
542   in development and disease. *Nat Rev Genet* **24**, 421-441, doi:10.1038/s41576-023-00587-9
543   (2023)PMC7615029.
544 26 Waters, A. M. & Beales, P. L. Ciliopathies: an expanding disease spectrum. *Pediatr Nephrol* **26**,
545   1039-1056, doi:10.1007/s00467-010-1731-7 (2011)3098370.
546 27 Guo, J. *et al.* Developmental disruptions underlying brain abnormalities in ciliopathies. *Nat*
547   *Commun* **6**, 7857, doi:10.1038/ncomms8857 (2015)PMC4515781.
548 28 Roosing, S. *et al.* Mutations in CEP120 cause Joubert syndrome as well as complex ciliopathy
549   phenotypes. *Journal of medical genetics* **53**, 608-615, doi:10.1136/jmedgenet-2016-103832
550   (2016)5013089.
551 29 Oh, E. C. & Katsanis, N. Cilia in vertebrate development and disease. *Development* **139**, 443-448,
552   doi:10.1242/dev.050054 (2012)3275291.
553 30 Sattar, S. & Gleeson, J. G. The ciliopathies in neuronal development: a clinical approach to
554   investigation of Joubert syndrome and Joubert syndrome-related disorders. *Dev Med Child*
555   *Neurol* **53**, 793-798, doi:10.1111/j.1469-8749.2011.04021.x (2011)PMC3984879.
556 31 Harris, P. C. & Torres, V. E. Genetic mechanisms and signaling pathways in autosomal dominant
557   polycystic kidney disease. *The Journal of clinical investigation* **124**, 2315-2324,
558   doi:10.1172/JCI72272 (2014)4089452.
559 32 Chebib, F. T., Sussman, C. R., Wang, X., Harris, P. C. & Torres, V. E. Vasopressin and disruption of
560   calcium signalling in polycystic kidney disease. *Nature reviews. Nephrology* **11**, 451-464,
561   doi:10.1038/nrneph.2015.39 (2015)4539141.
562 33 Mirra, V., Werner, C. & Santamaria, F. Primary Ciliary Dyskinesia: An Update on Clinical Aspects,
563   Genetics, Diagnosis, and Future Treatment Strategies. *Frontiers in pediatrics* **5**, 135,
564   doi:10.3389/fped.2017.00135 (2017)5465251.
565 34 Helou, J. *et al.* Mutation analysis of NPHP6/CEP290 in patients with Joubert syndrome and
566   Senior-Loken syndrome. *J Med Genet* **44**, 657-663, doi:10.1136/jmg.2007.052027
567   (2007)PMC2597962.
568 35 Ta, C. M., Vien, T. N., Ng, L. C. T. & DeCaen, P. G. Structure and function of polycystin channels in
569   primary cilia. *Cell Signal* **72**, 109626, doi:10.1016/j.cellsig.2020.109626 (2020)PMC7373203.
570 36 Su, S. *et al.* Genetically encoded calcium indicator illuminates calcium dynamics in primary cilia.
571   *Nat Methods* **10**, 1105-1107, doi:10.1038/nmeth.2647 (2013)PMC3860264.

572 37   Delling, M., DeCaen, P. G., Doerner, J. F., Febvay, S. & Clapham, D. E. Primary cilia are specialized
573   calcium signalling organelles. *Nature* **504**, 311-314, doi:10.1038/nature12833 (2013)4112737.
574 38   Jiang, J. Y., Falcone, J. L., Curci, S. & Hofer, A. M. Direct visualization of cAMP signaling in primary
575   cilia reveals up-regulation of ciliary GPCR activity following Hedgehog activation. *Proc Natl Acad*
576   *Sci U S A* **116**, 12066-12071, doi:10.1073/pnas.1819730116 (2019)PMC6575585.
577 39   Pazour, G. J., San Agustin, J. T., Follit, J. A., Rosenbaum, J. L. & Witman, G. B. Polycystin-2
578   localizes to kidney cilia and the ciliary level is elevated in orpk mice with polycystic kidney
579   disease. *Curr Biol* **12**, R378-380, doi:10.1016/s0960-9822(02)00877-1 (2002)
580 40   Kleene, S. J. & Kleene, N. K. The native TRPP2-dependent channel of murine renal primary cilia.
581   *Am J Physiol Renal Physiol* **312**, F96-F108, doi:10.1152/ajprenal.00272.2016 (2017)5283891.
582 41   DeCaen, P. G., Delling, M., Vien, T. N. & Clapham, D. E. Direct recording and molecular
583   identification of the calcium channel of primary cilia. *Nature* **504**, 315-318,
584   doi:10.1038/nature12832 (2013)PMC4073646.
585 42   Liu, X. *et al.* Polycystin-2 is an essential ion channel subunit in the primary cilium of the renal
586   collecting duct epithelium. *Elife*, doi:10.1101/215814 (2017)
587 43   Neher, E. & Sakmann, B. Noise analysis of drug induced voltage clamp currents in denervated
588   frog muscle fibres. *J Physiol* **258**, 705-729, doi:10.1113/jphysiol.1976.sp011442
589   (1976)PMC1309001.
590 44   Cramer, T. M. L. & Tyagarajan, S. K. Protocol for the culturing of primary hippocampal mouse
591   neurons for functional in vitro studies. *STAR Protoc* **5**, 102991, doi:10.1016/j.xpro.2024.102991
592   (2024)PMC11017351.
593 45   Liu, C. & Hermann, T. E. Characterization of ionomycin as a calcium ionophore. *J Biol Chem* **253**,
594   5892-5894 (1978)
595 46   Babic Leko, M. *et al.* Serotonin Receptor Gene Polymorphisms Are Associated with
596   Cerebrospinal Fluid, Genetic, and Neuropsychological Biomarkers of Alzheimer's Disease.
597   *Biomedicines* **10**, doi:10.3390/biomedicines10123118 (2022)PMC9775360.
598 47   Chiu, H. J. *et al.* Serotonin 6 receptor polymorphism in schizophrenia: frequency, age at onset
599   and cognitive function. *Neuropsychobiology* **43**, 113-116, doi:10.1159/000054876 (2001)
600 48   Halls, M. L. & Cooper, D. M. Regulation by Ca2+-signaling pathways of adenylyl cyclases. *Cold*
601   *Spring Harb Perspect Biol* **3**, a004143, doi:10.1101/cshperspect.a004143 (2011)PMC3003456.
602 49   Sanchez, G. M. *et al.* The beta-cell primary cilium is an autonomous Ca2+ compartment for
603   paracrine GABA signaling. *J Cell Biol* **222**, doi:10.1083/jcb.202108101 (2023)PMC9813980.
604 50   Winans, A. M. *et al.* Ciliary localization of a light-activated neuronal GPCR shapes behavior. *Proc*
605   *Natl Acad Sci U S A* **120**, e2311131120, doi:10.1073/pnas.2311131120 (2023)PMC10614621.
606 51   Hansen, J. N. *et al.* Nanobody-directed targeting of optogenetic tools to study signaling in the
607   primary cilium. *Elife* **9**, doi:10.7554/eLife.57907 (2020)PMC7338050.
608 52   Truong, M. E. *et al.* Vertebrate cells differentially interpret ciliary and extraciliary cAMP. *Cell* **184**,
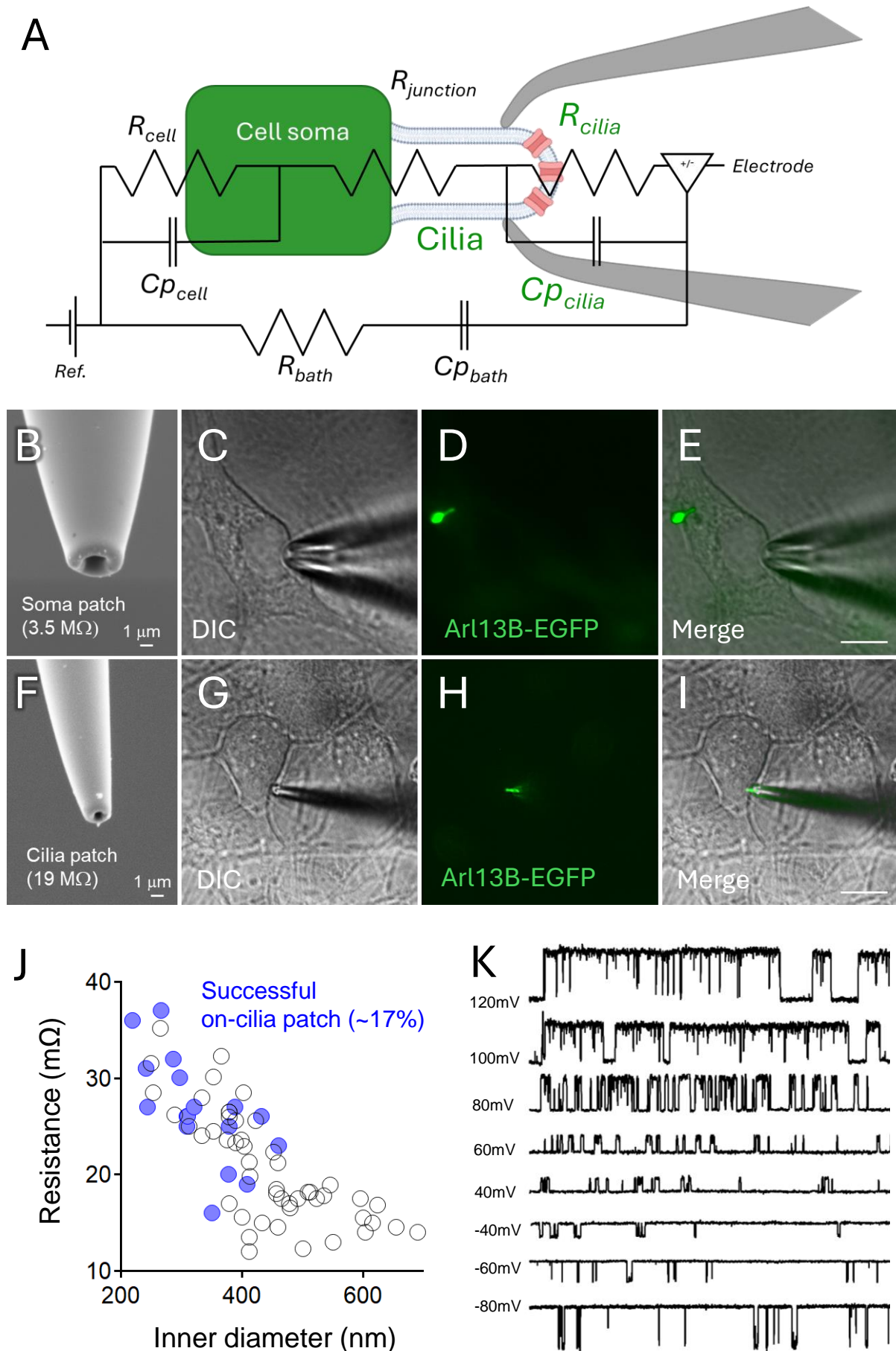609   2911-2926 e2918, doi:10.1016/j.cell.2021.04.002 (2021)PMC8450001.
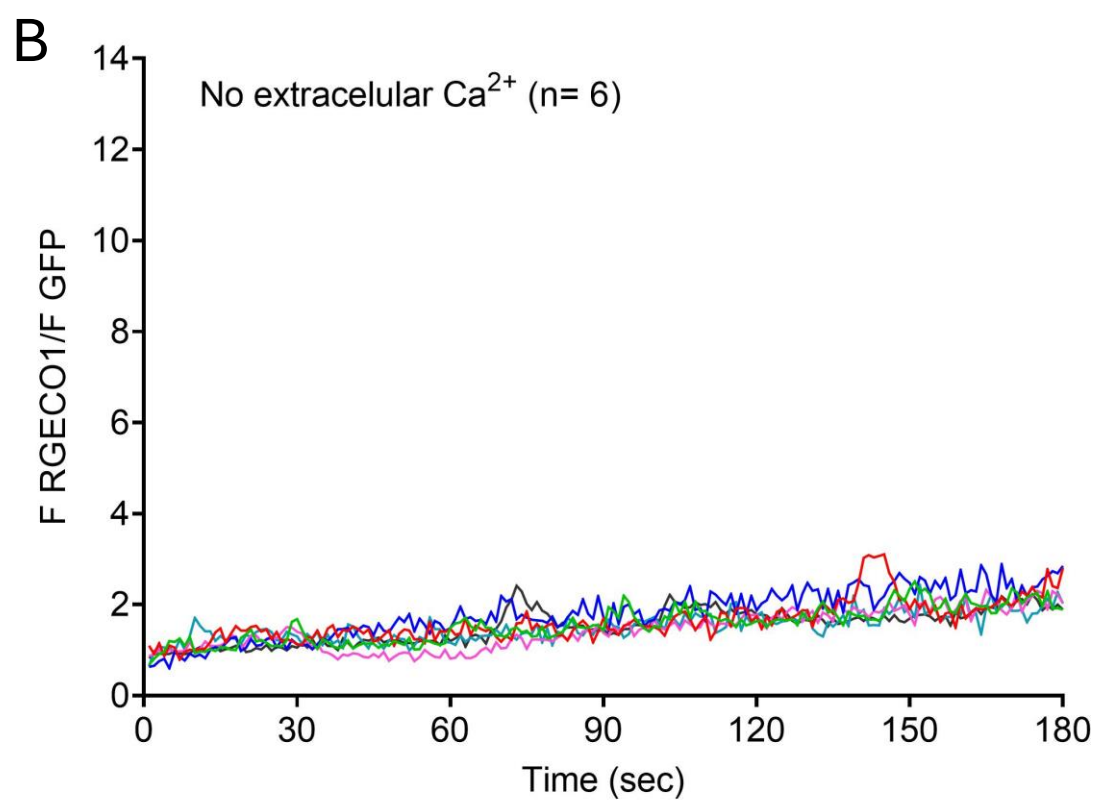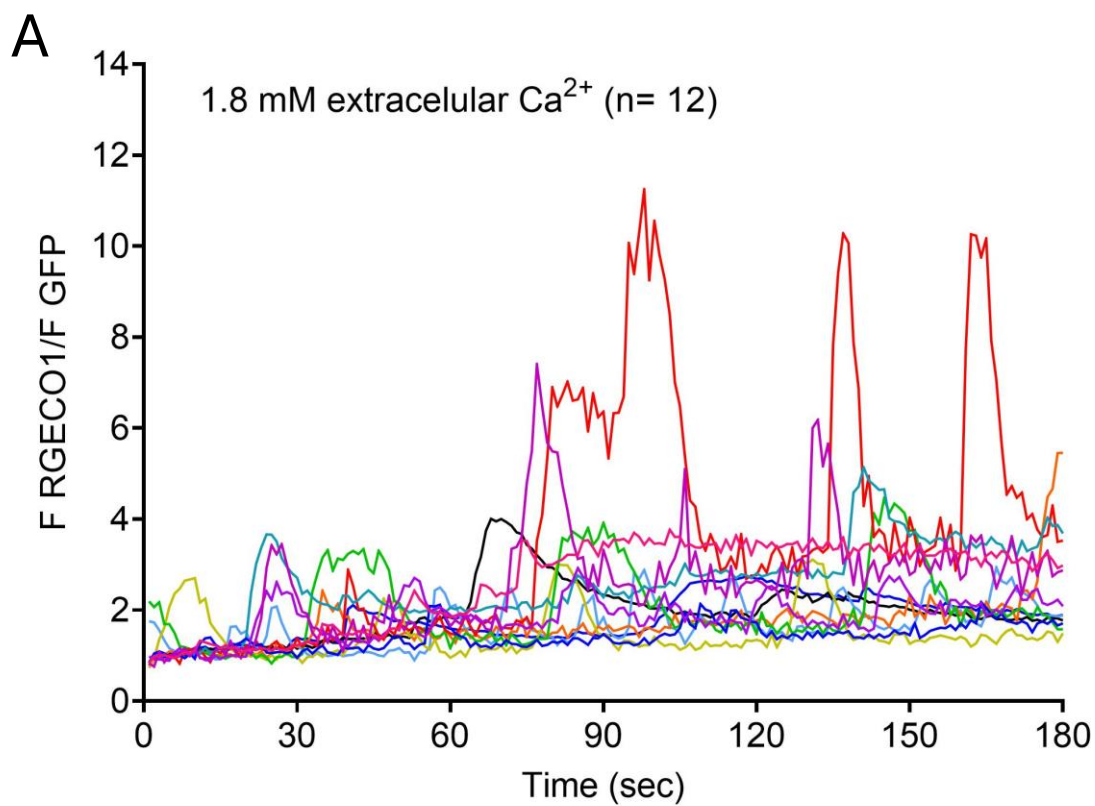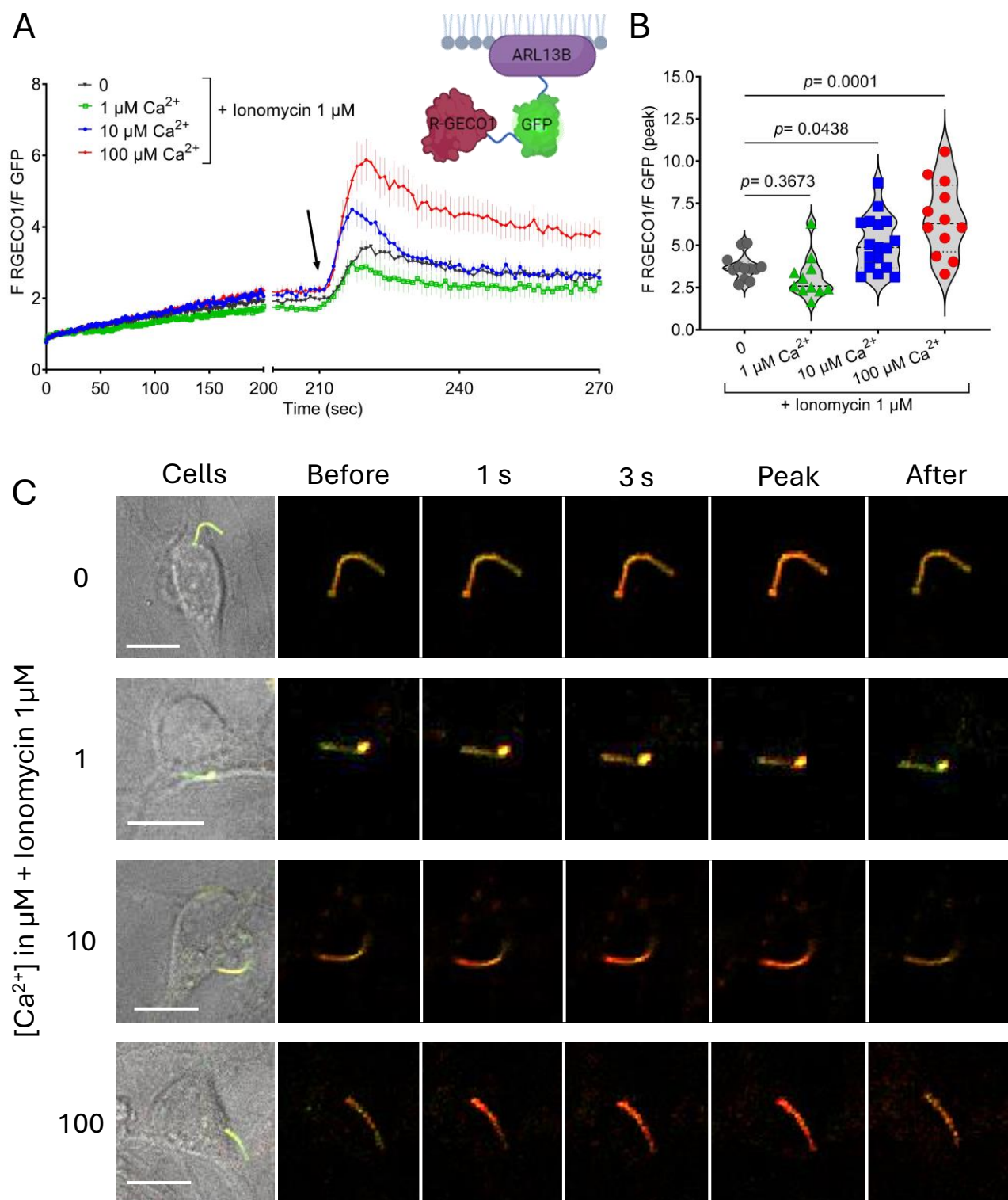
610

Figure 1

Figure 2

Figure 3

Figure 4

A   4 h

B   DIV 1

C   DIV 6

D   DIV 9

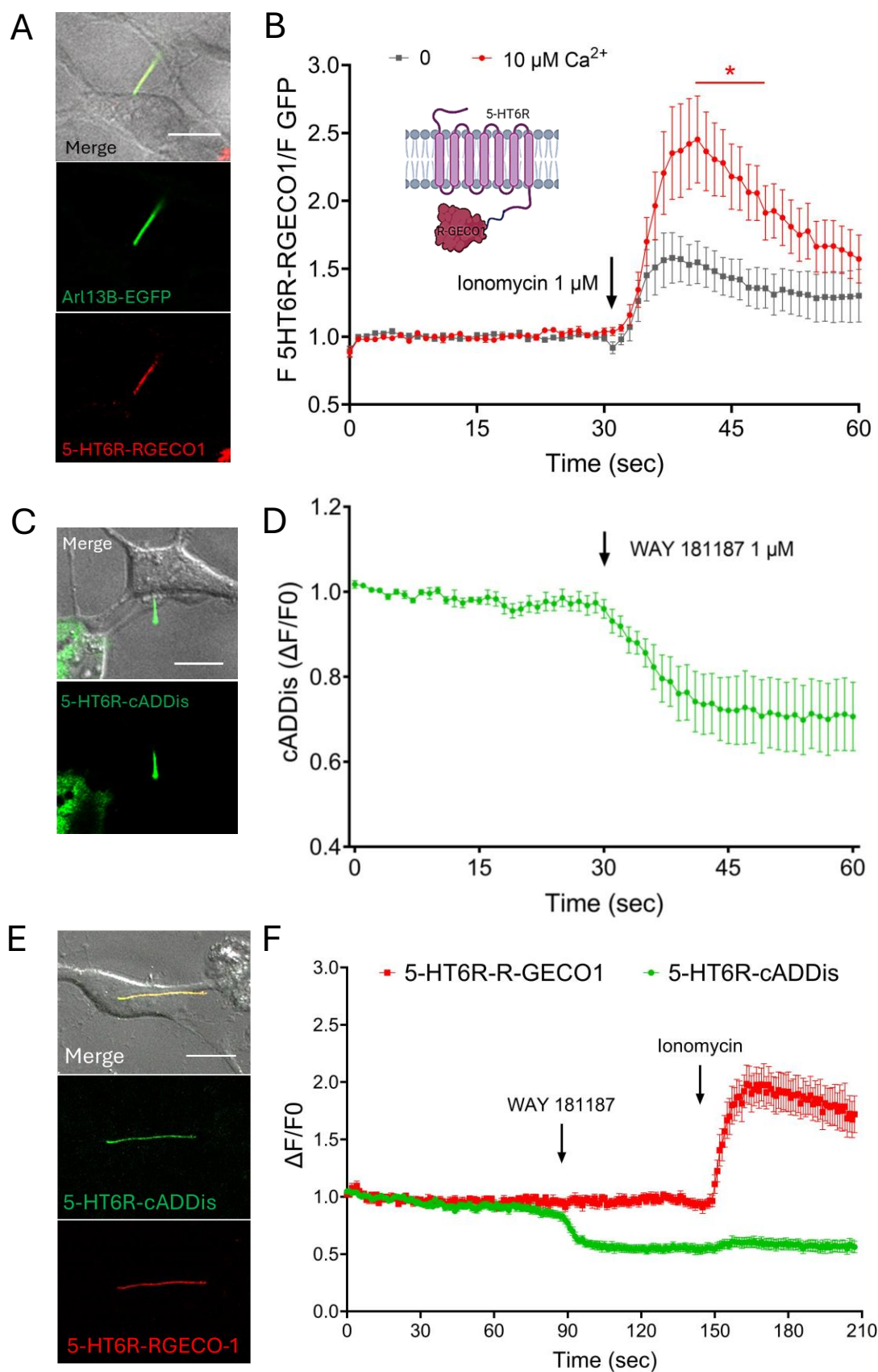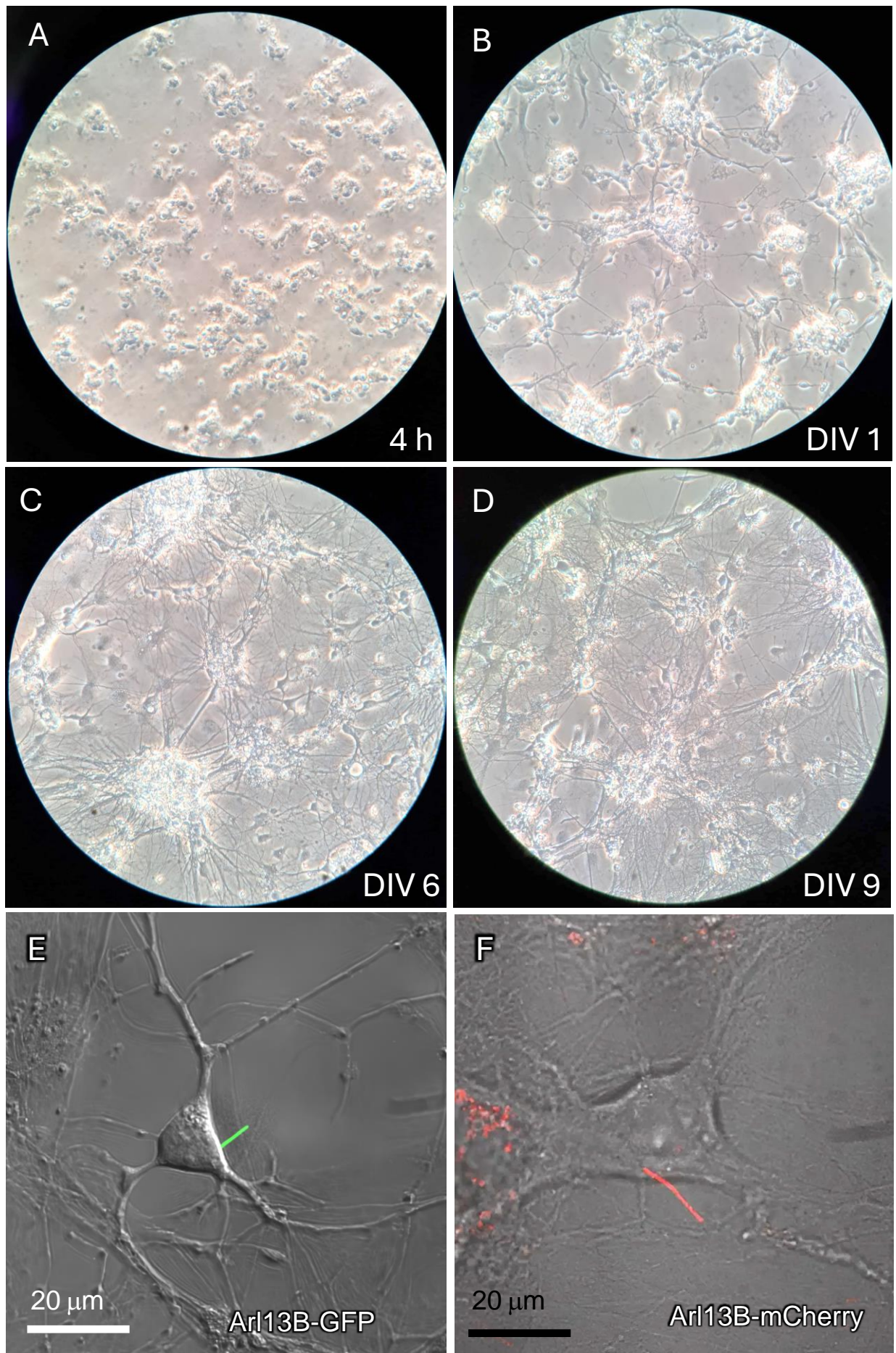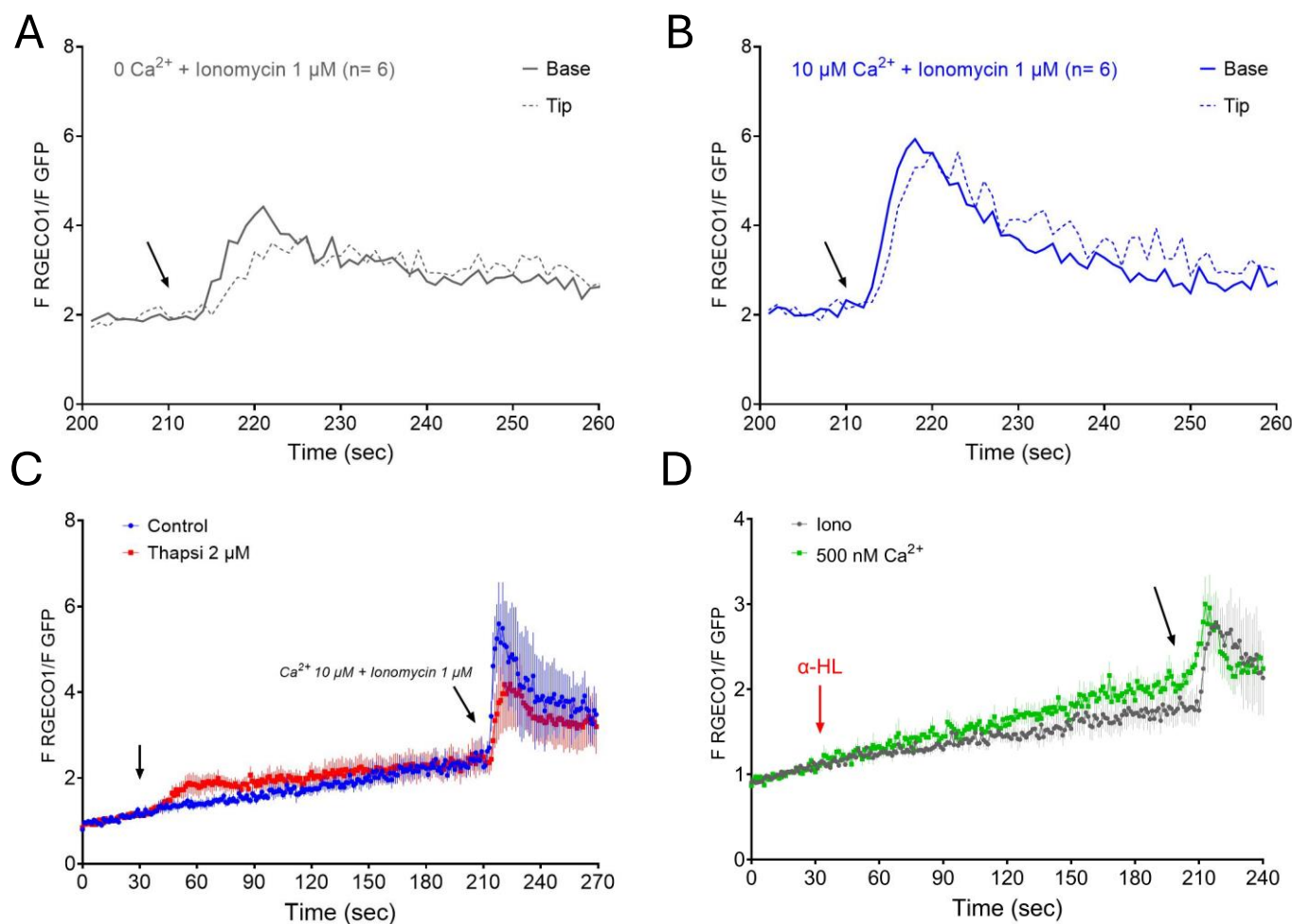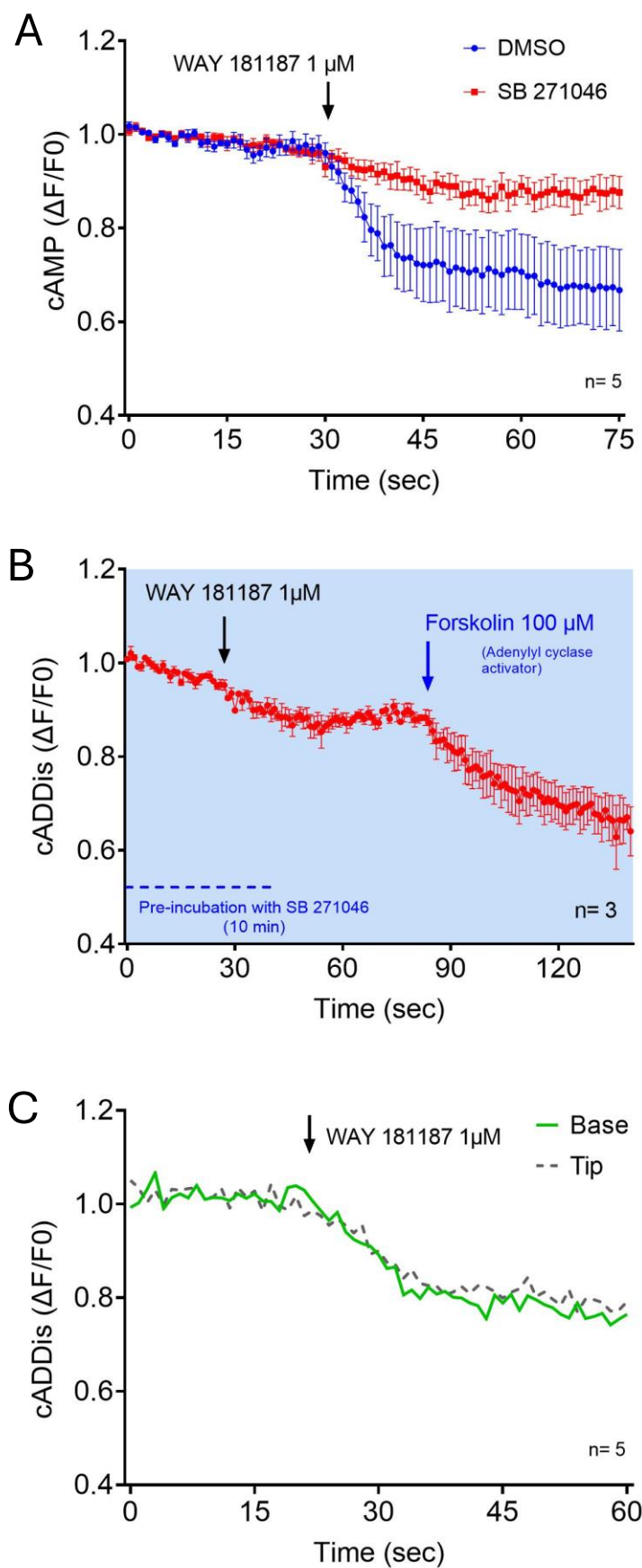E   20 μm   Arl13B-GFP

F   20 μm   Arl13B-mCherry

Supplemental Figure 1

Supplemental Figure 2

Supplemental Figure 3